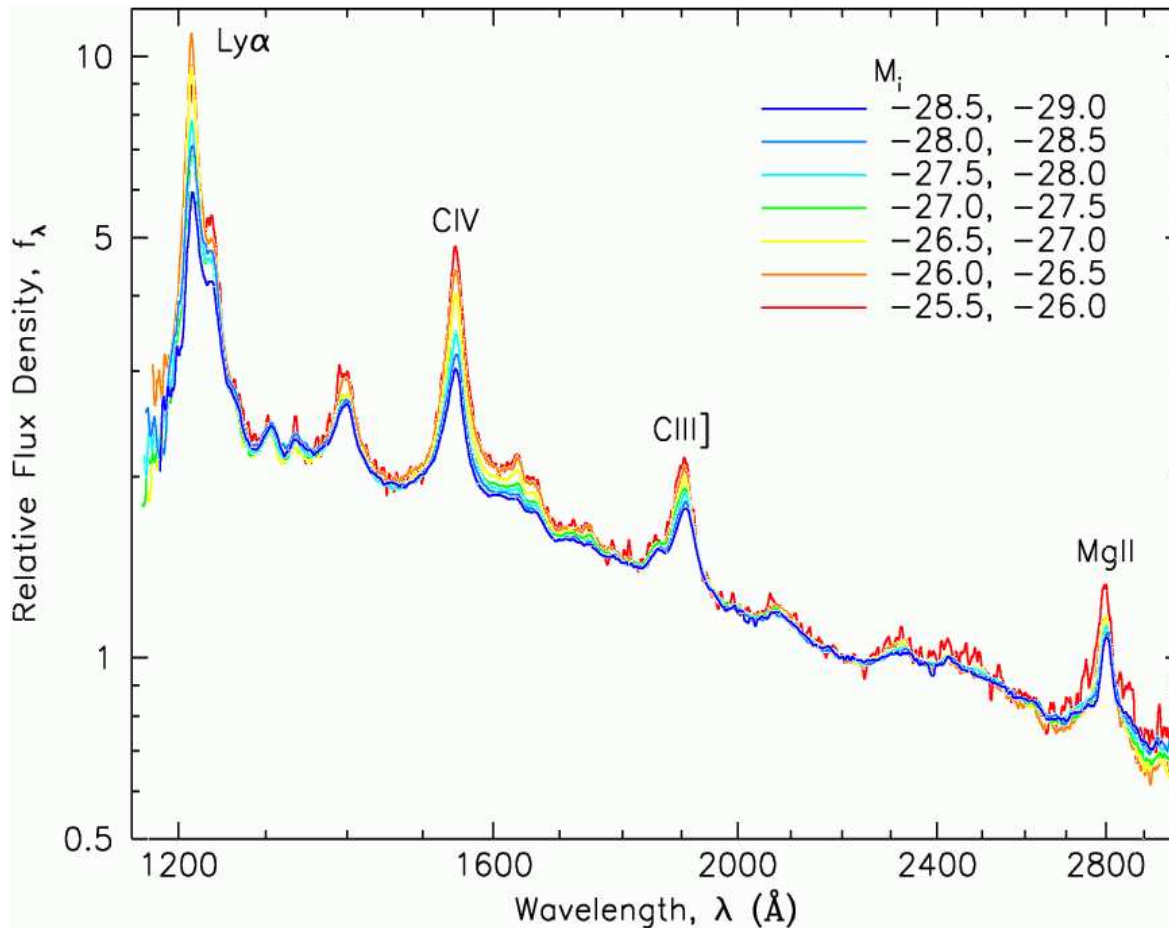




Broad Line Region



Introduction



Average quasar spectra for $2.03 < z < 2.311$, normalized to the same flux at $\lambda = 2200\text{\AA}$ (vanden Berk et al., 2004, Fig. 1)

Review: Peterson (2006)

- Overall, *spectral shape* is *luminosity independent*
- **Baldwin effect**: Emission lines (esp. Ly α and C IV 1549 \AA) weaker in more luminous objects, although shape similar.

This chapter: *physics of region emitting the broad lines.*



Properties

General properties of the BLR from observed spectrum:

- Emission lines from BLR: **typical for $T \sim 10^4$ K** (photoionization)
- **Lines have widths of $500 \dots 25000 \text{ km s}^{-1}$**

Thermal motion:

$$E_{\text{kin}} = \frac{1}{2} m_p v^2 = \frac{3}{2} kT \quad (8.1)$$

\implies **Typical thermal speed:**

$$v \sim \sqrt{\frac{3kT}{m_p}} \sim 20 \text{ km s}^{-1} \quad (8.2)$$

- Line broadening is due to **supersonic bulk motion** of BLR emitting gas
- No [O III] 4959/5007 lines $\implies n \gtrsim n_{\text{crit}, 5077} \sim 10^8 \text{ cm}^{-3}$.
- C iii] 1909 line sometimes broad, so $n \lesssim n_{\text{crit}, 1909} \sim 10^{10} \text{ cm}^{-3}$.

More detailed analyses show C iii] to originate in region different from Ly α emitting region, typical densities can be as high as 10^{11} cm^{-3} .



Location

Location of BLR from line width:

Assume emitting gas on a circular orbit:

Kepler speed:

$$\frac{mv^2}{r} = \frac{GMm}{r^2} \implies v = \sqrt{\frac{GM}{r}} \quad (8.3)$$

such that

$$r = \frac{GM}{v^2} = 3600 \text{ AU} \left(\frac{M}{10^6 M_{\odot}} \right) \left(\frac{v}{500 \text{ km s}^{-1}} \right)^{-2} \quad (8.4)$$

The BLR is located **close** to the central black hole.

Note: BLR probably does *not* consist of gas on circular orbits around the BH, so real size is larger.



BLR: Mass

Mass determination: Determine number of emitting atoms from line strength, e.g., H β (less influenced by radiative transfer effects than Lyman lines)

Line emissivity:

$$j_{\text{H}\beta} = n_e n_p \alpha_{\text{H}\beta} \frac{h\nu_{\text{H}\beta}}{4\pi} = n_e^2 \alpha_{\text{H}\beta}^{\text{eff}} \frac{h\nu_{\text{H}\beta}}{4\pi} = 1.24 \times 10^{-25} \text{ erg s}^{-1} \text{ cm}^{-3} \text{ sr}^{-1} \frac{n_e^2}{4\pi} \quad (8.5)$$

where $\alpha_{\text{H}\beta}^{\text{eff}}$: effective recombination coefficient for $n = 4 \rightarrow n = 2$ transition (weakly temperature dependent).

Total H β luminosity:

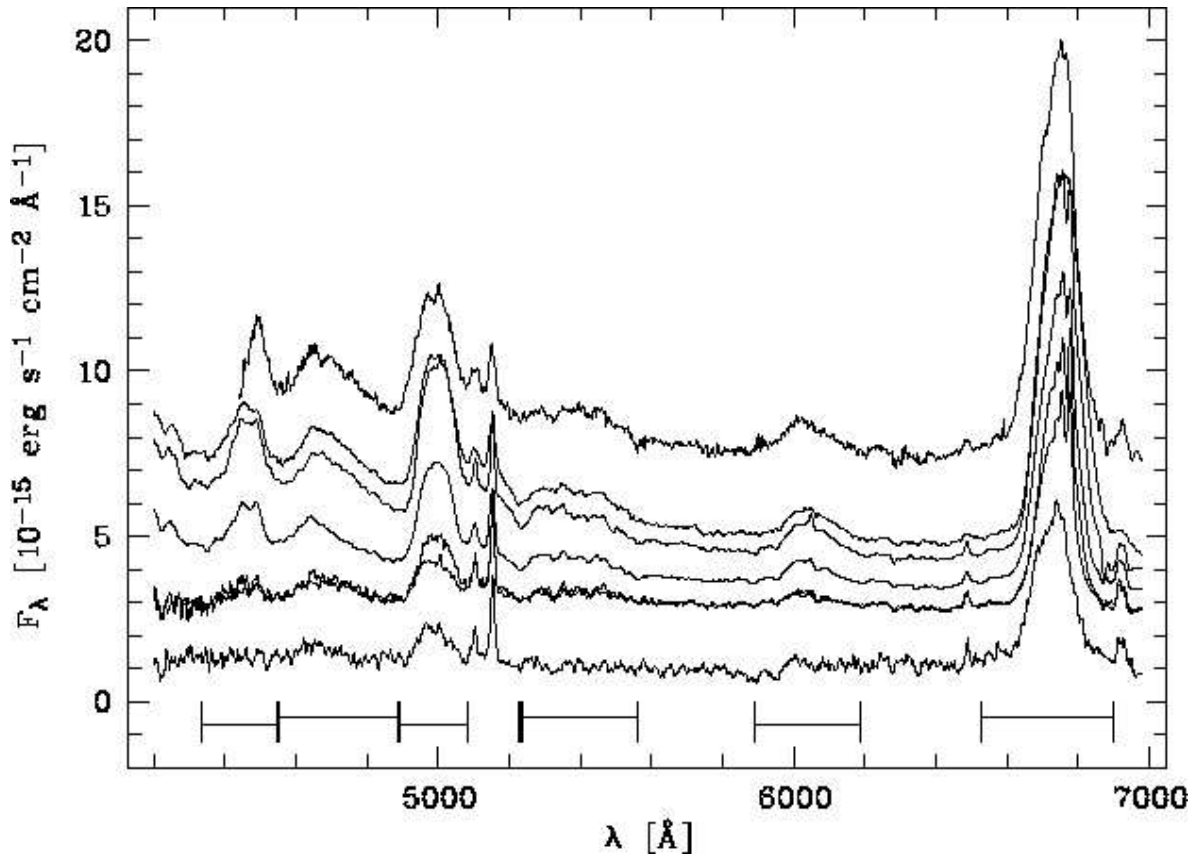
$$L_{\text{H}\beta} = \iint j_{\text{H}\beta} d\Omega dV = \frac{4\pi n_e^2}{3} \cdot 1.24 \times 10^{-25} r^3 f \text{ erg s}^{-1} \propto \int n_e^2 dV \quad (8.6)$$

where $\int n_e^2 dV$: **emission measure**, and f : **filling factor**.

BLR lines give BLR mass of $\sim 1 M_{\odot}$ and $f \sim 10^{-3}$.

Observed lines are bright because of n^2 -proportionality and high density of BLR gas.

BLR Line Variability, I

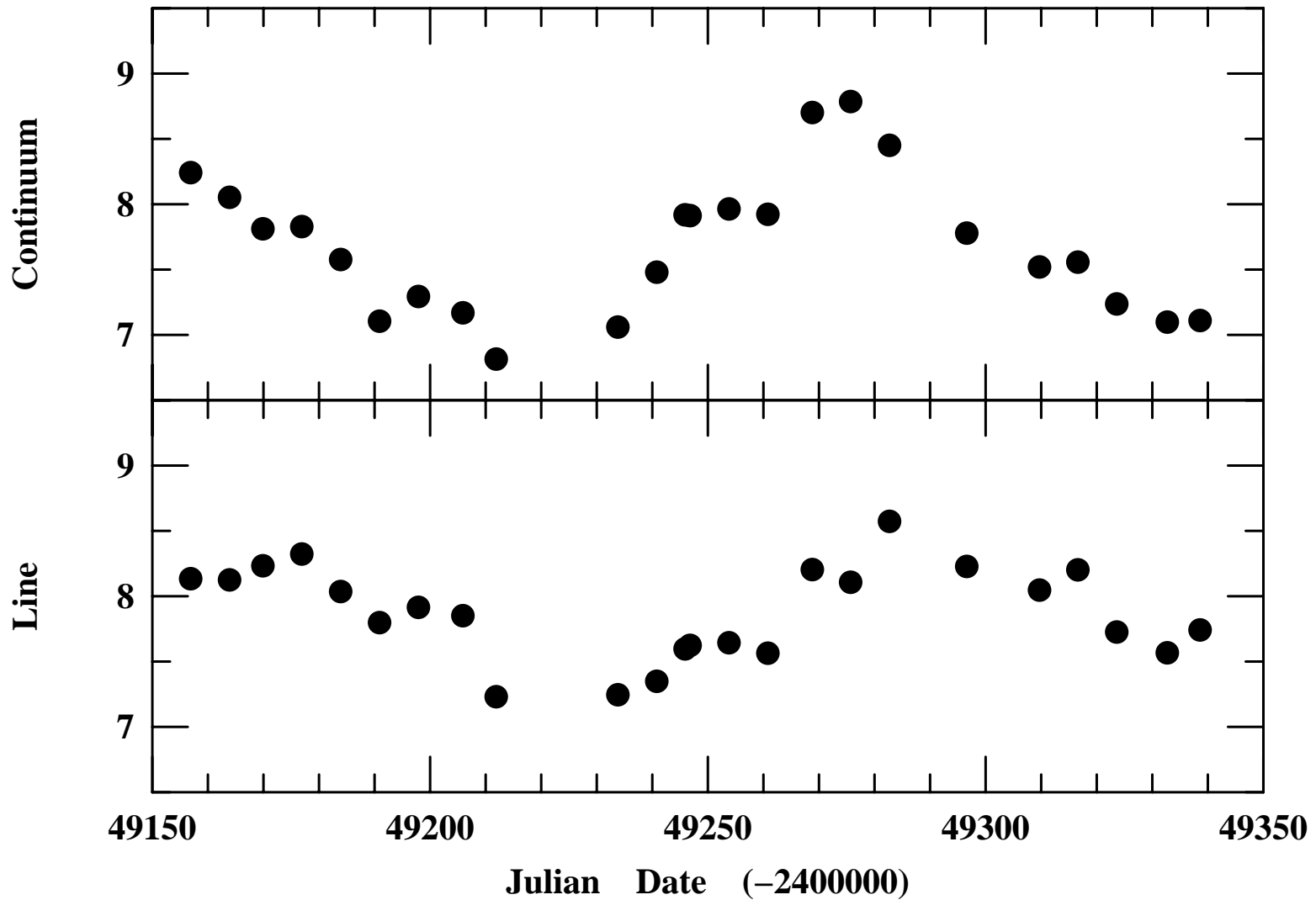


Broad lines are variable on timescales from days to years.

Spectral variability of NGC 7603 (Sy 1), top to bottom: Dec 98, Dec 93, Sep 93, Aug 92, Jul 90, Oct 88, and Oct 79 (Kollatschny, Bischoff & Dietrich, 2000, Fig. 2)

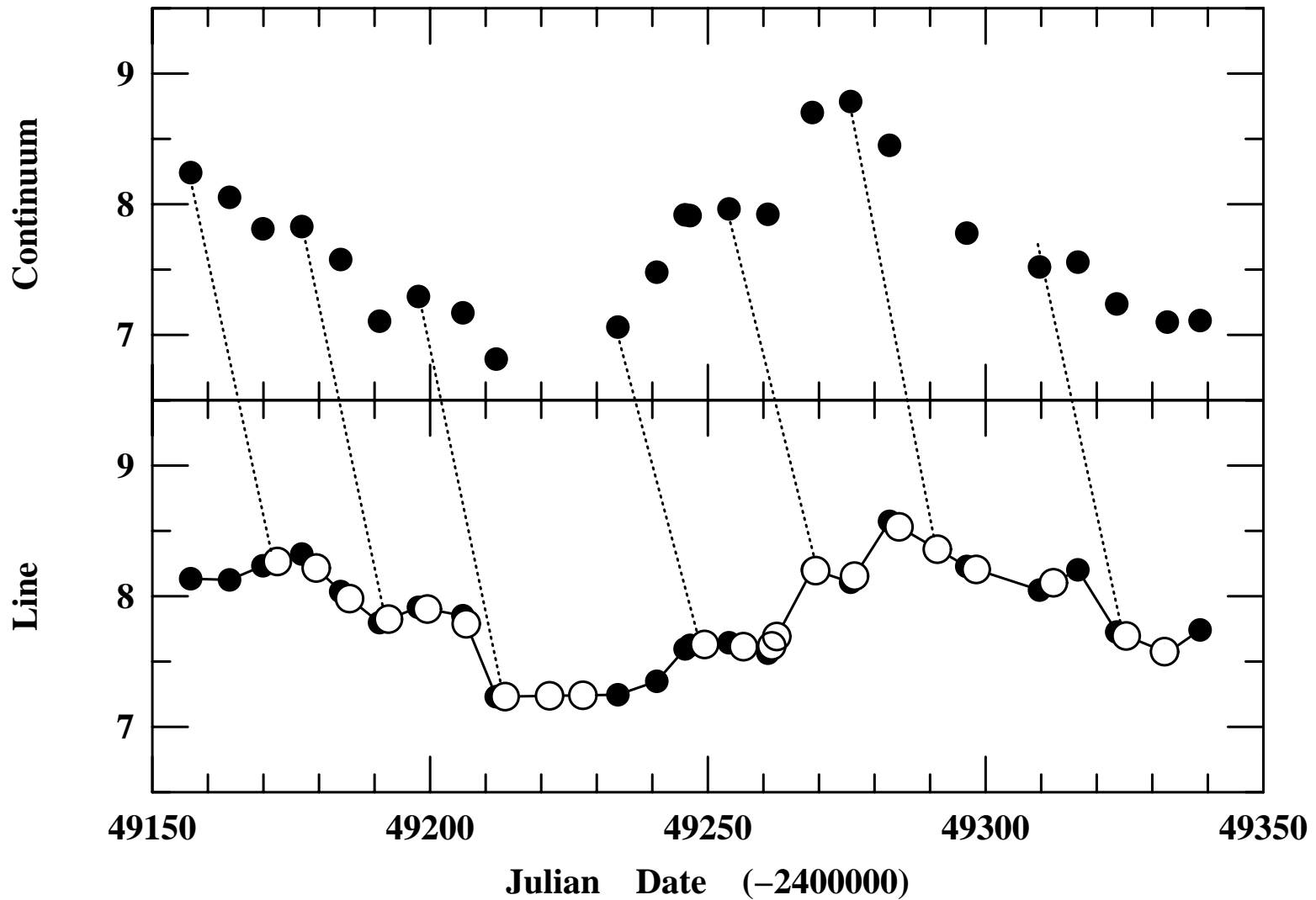


BLR Line Variability, II

Continuum and $H\beta$ fluxes for Mkn 335 (Peterson, 2001, Fig. 23)



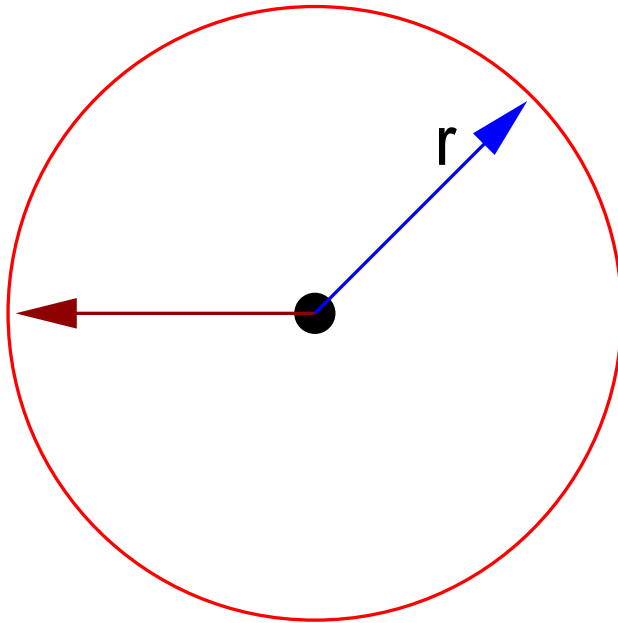
BLR Line Variability, III



Mkn 335: $H\beta$ line lags continuum by 15.6 d (Peterson, 2001, Fig. 24)



Reverberation Mapping



AGN time variability helps to map gas around Black Hole.

Flash at time $t = 0$ will illuminate gas at distance r after **time delay**

$$\tau = r/c \quad (8.7)$$

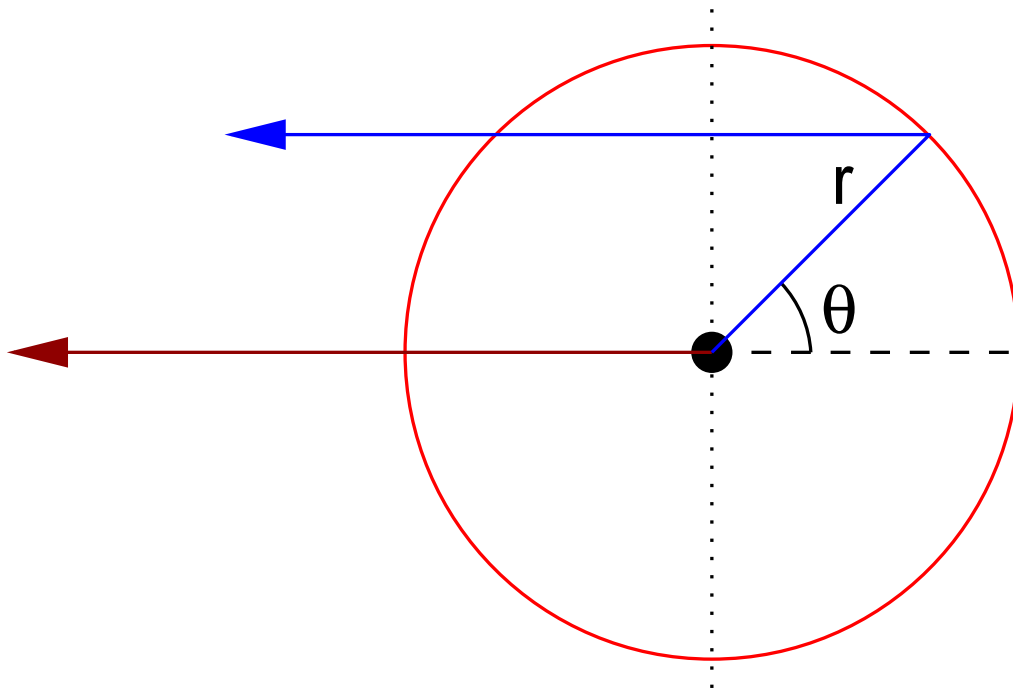
Gas is ionized by flash. **Recombination timescale** of gas is

$$\tilde{\tau} = \frac{1}{n_e \alpha} \sim 40 n_{11}^{-1} \text{ s} \quad (8.8)$$

i.e., “quasi instantaneous”.



Reverberation Mapping



Light emitted by illuminated gas will be observed only after a **time delay**.

Extra distance traveled by light from r :

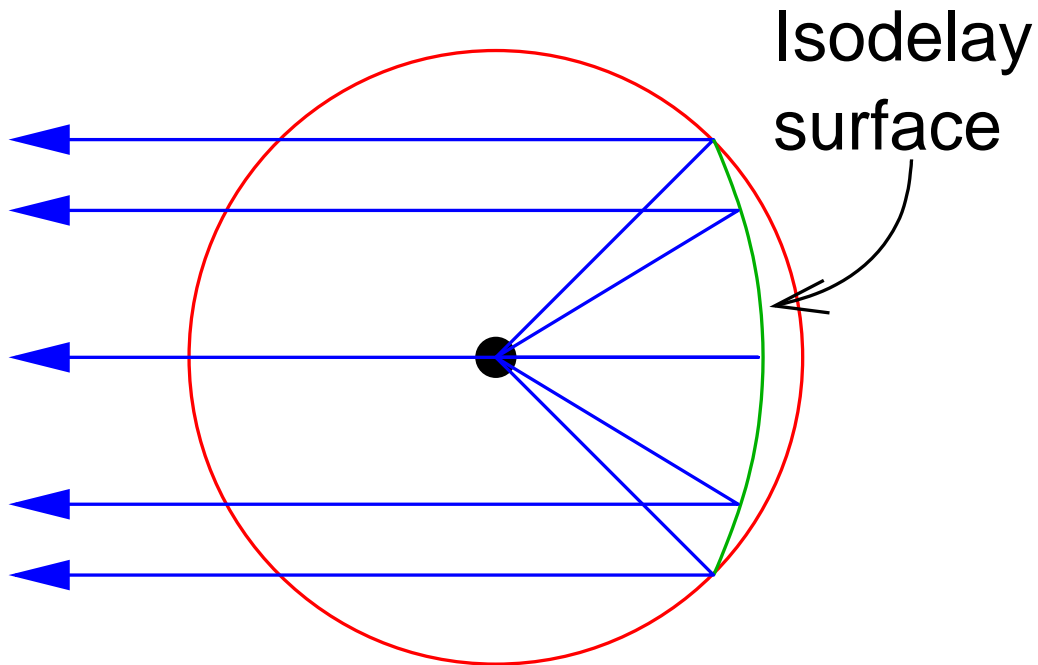
$$r' = r + r \cos \theta \quad (8.9)$$

Time delay due to light travel effect:

$$\tau = (1 + \cos \theta) \frac{r}{c} \quad (8.10)$$



Reverberation Mapping



Time delay was given by:

$$\tau = (1 + \cos \theta) \frac{r}{c} \quad (8.10)$$

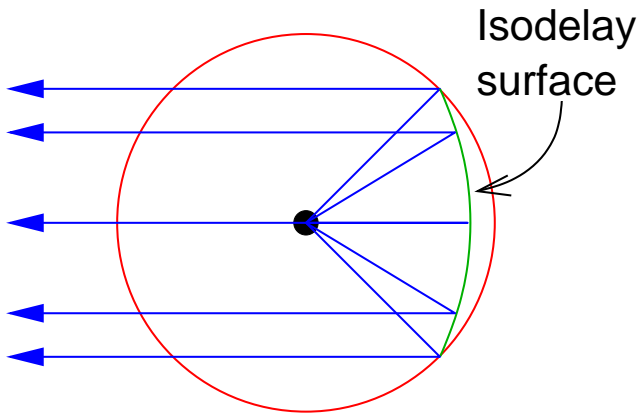
Locus of points with same time delay (**isodelay surface**):

$$r(\tau) = \frac{c\tau}{1 + \cos \theta} \quad (8.11)$$

(i.e., a **parabola**)



Reverberation Mapping



Assume that line intensity increases by factor ζ when BLR gas is illuminated by flash.

\implies **total line emissivity increase** from the isodelay surface:

$$\Psi(\theta)d\theta = \zeta \cdot 2\pi r^2 \sin\theta d\theta \quad (8.12)$$

This assumes that conditions in BLR at r are the same everywhere.

$\Psi(r)d\theta$ corresponds to a **response at time delay τ** :

$$\Psi(\tau)d\tau = \Psi(\theta)d\theta \left| \frac{d\theta}{d\tau} \right| d\tau = \zeta \cdot 2\pi r^2 \sin\theta \cdot \frac{c}{r \sin\theta} d\tau = 2\pi\zeta r c d\tau \quad (8.13)$$

where $\tau = (1 + \cos\theta)r/c$, i.e., $d\tau/d\theta = -\sin\theta \cdot r/c$ was used.



Reverberation Mapping

In reality, AGN does not emit shots, but nucleus varies stochastically \implies

Reverberation mapping (Blandford & McKee, 1982)

Describe continuum variability as $C(t)$.

Observed line variability, L , is:

$$L(t) = \int_{-\infty}^{+\infty} \Psi(\tau) C(t - \tau) d\tau \quad (8.14)$$

(“**convolution**” of C with kernel $\Psi(\tau)$).

Observational problem is the inverse of Eq. (8.14): **Given $L(t)$, determine $\Psi(\tau)$.**

($C(t - \tau)$ is known from continuum variations), provided the lightcurve is long enough, as τ can be days to months!



Reverberation Mapping

To solve equations such as

$$L(t) = \int_{-\infty}^{+\infty} \Psi(\tau)C(t - \tau)d\tau \quad (8.14)$$

for Ψ , the standard approach in mathematics is to determine the **Fourier transform** of $L(t)$:

$$L(f) = \int_{-\infty}^{+\infty} L(t)e^{-2\pi ift}dt \quad (8.15)$$

inserting Eq. (8.14) gives

$$= \int_{-\infty}^{+\infty} \int_{-\infty}^{+\infty} \Psi(\tau)C(t - \tau)e^{-2\pi ift}d\tau dt \quad (8.16)$$

change order of integration

$$= \int_{-\infty}^{+\infty} \Psi(\tau) \int_{-\infty}^{+\infty} C(t - \tau)e^{-2\pi ift}dt d\tau \quad (8.17)$$

substitute $t - \tau \longrightarrow t'$

$$= \int_{-\infty}^{+\infty} \Psi(\tau) \int_{-\infty}^{+\infty} C(t')e^{-2\pi if(t'+\tau)}dt' d\tau \quad (8.18)$$



Reverberation Mapping

Therefore

$$L(f) = \int_{-\infty}^{+\infty} \Psi(\tau) \int_{-\infty}^{+\infty} C(t') e^{-2\pi i f(t'+\tau)} dt' d\tau \quad (8.18)$$

move constant outside of the inner integral and drop the prime

$$= \int_{-\infty}^{+\infty} \Psi(\tau) e^{-2\pi i f\tau} \int_{-\infty}^{+\infty} C(t) e^{-2\pi i ft} dt d\tau \quad (8.19)$$

since the inner integral is a constant this gives

$$= \int_{-\infty}^{+\infty} e^{-2\pi i f\tau} \Psi(\tau) d\tau \cdot \int_{-\infty}^{+\infty} C(t) e^{-2\pi i ft} dt \quad (8.20)$$

which is the product of the Fourier transforms of C and Ψ :

$$L(f) = \Psi(f) \cdot C(f) \quad (8.21)$$

The Fourier transform of L is the product of the Fourier transforms of Ψ and C .

This is just the **convolution theorem** of Fourier theory.



Reverberation Mapping

Blandford & McKee (1982): Since $L(f)$ and $C(f)$ can be measured, we can determine $\Psi(f)$ and then do an inverse FT:

$$\Psi(t) = \frac{1}{2\pi} \int_{-\infty}^{+\infty} \Psi(f) e^{+2\pi i f t} df \quad (8.22)$$

so we can in principle measure $\Psi(f)$.

In practice: **Fourier approach does not work.**

Reason: **Sparse sampling of lightcurves**

⇒ Potential of reverberation mapping has not yet been realized!

What *is* possible is to **determine size of BLR from reverberation mapping**



Reverberation Mapping

To get BLR size from reverberation, **work in time domain** and determine **cross correlation** of $L(t)$ and $C(t)$:

$$\text{CCF}(\tau) = \int_{-\infty}^{+\infty} L(t)C(t - \tau)dt \quad (8.23)$$

insert $L(t)$ from Eq. (8.14):

$$= \int_{-\infty}^{+\infty} C(t - \tau) \int_{-\infty}^{+\infty} C(t - \tau')\Psi(\tau')d\tau' dt \quad (8.24)$$

change order of integration

$$= \int_{-\infty}^{+\infty} \Psi(\tau') \int_{-\infty}^{+\infty} C(t - \tau)C(t - \tau')dt d\tau' \quad (8.25)$$

and introduce the **auto correlation function**, ACF,

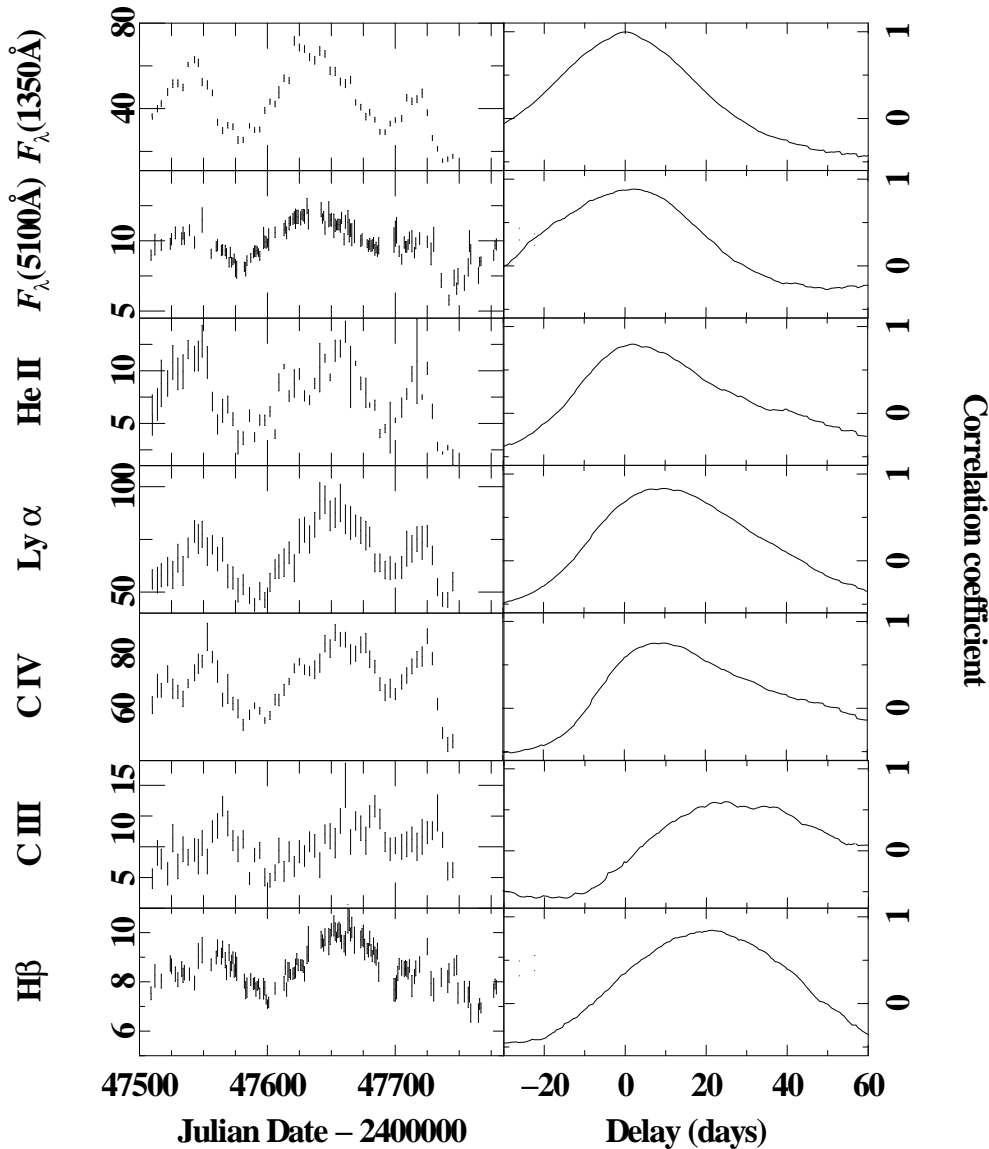
$$= \int_{-\infty}^{+\infty} \Psi(\tau')\text{ACF}(\tau - \tau')d\tau' \quad (8.26)$$

where

$$\text{ACF}(\tau) = \int_{-\infty}^{+\infty} C(t)C(t - \tau)dt \quad (8.27)$$



Reverberation Mapping



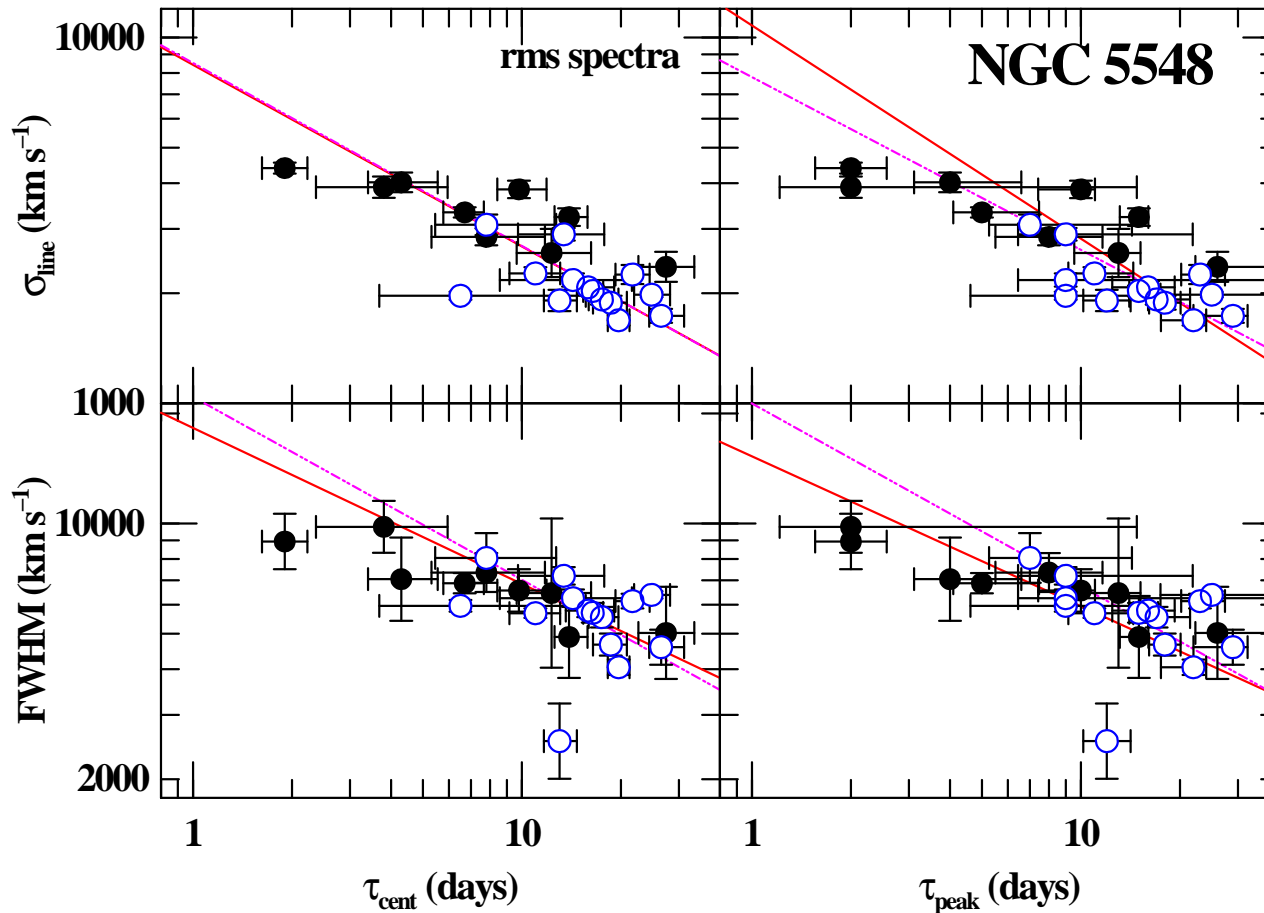
CCF has a peak at the lag for which $C(t)$ and $L(t)$ match best

\Rightarrow Based on the CCF we can measure the size of the BLR.

In practice, one has to interpolate $C(t)$ and $L(t)$ to determine CCF using a discretized version of the integrals shown previously.

Light curves and CCFs with respect to 1350Å UV continuum for NGC 5548 (Clavel et al., 1992; Peterson, 2001).

Reverberation Mapping



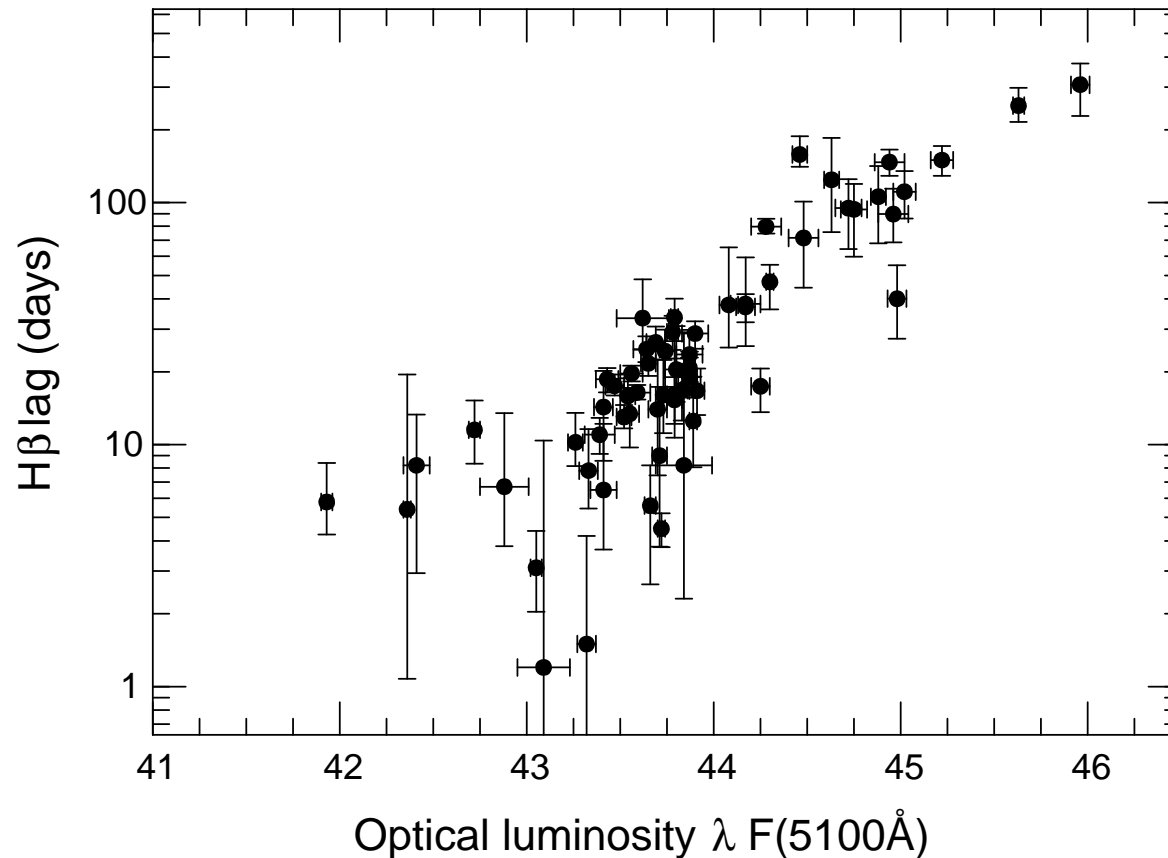
(Peterson et al., 2004, Fig. 3)

As expected: **broadest lines vary fastest.**

Also found: **higher ionization lines vary fastest** \implies **BLR has stratified ionization structure**



Reverberation Mapping



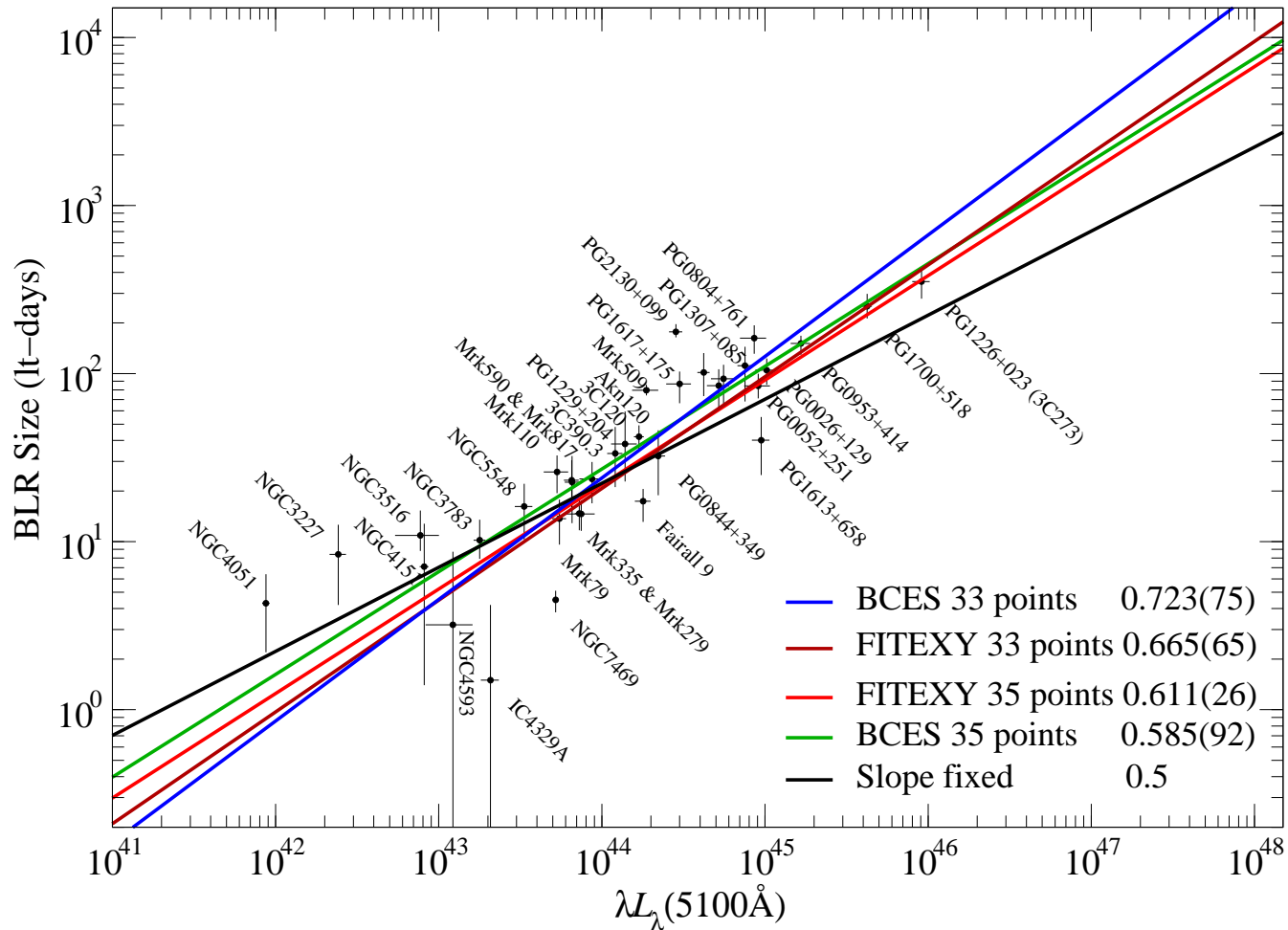
(Peterson, 2006, Fig. 6)

The photoionization parameter was $U \propto L/(D^2 n_e)$ (Eq. 7.20) so for U , n_e constant, we expect $D \propto L^{0.5}$. This is roughly what is observed!

$U = \text{const.}$ is expected since AGN spectra are all similar, so conditions in BLR are similar everywhere (“locally optimally emitting clouds”).



Reverberation Mapping



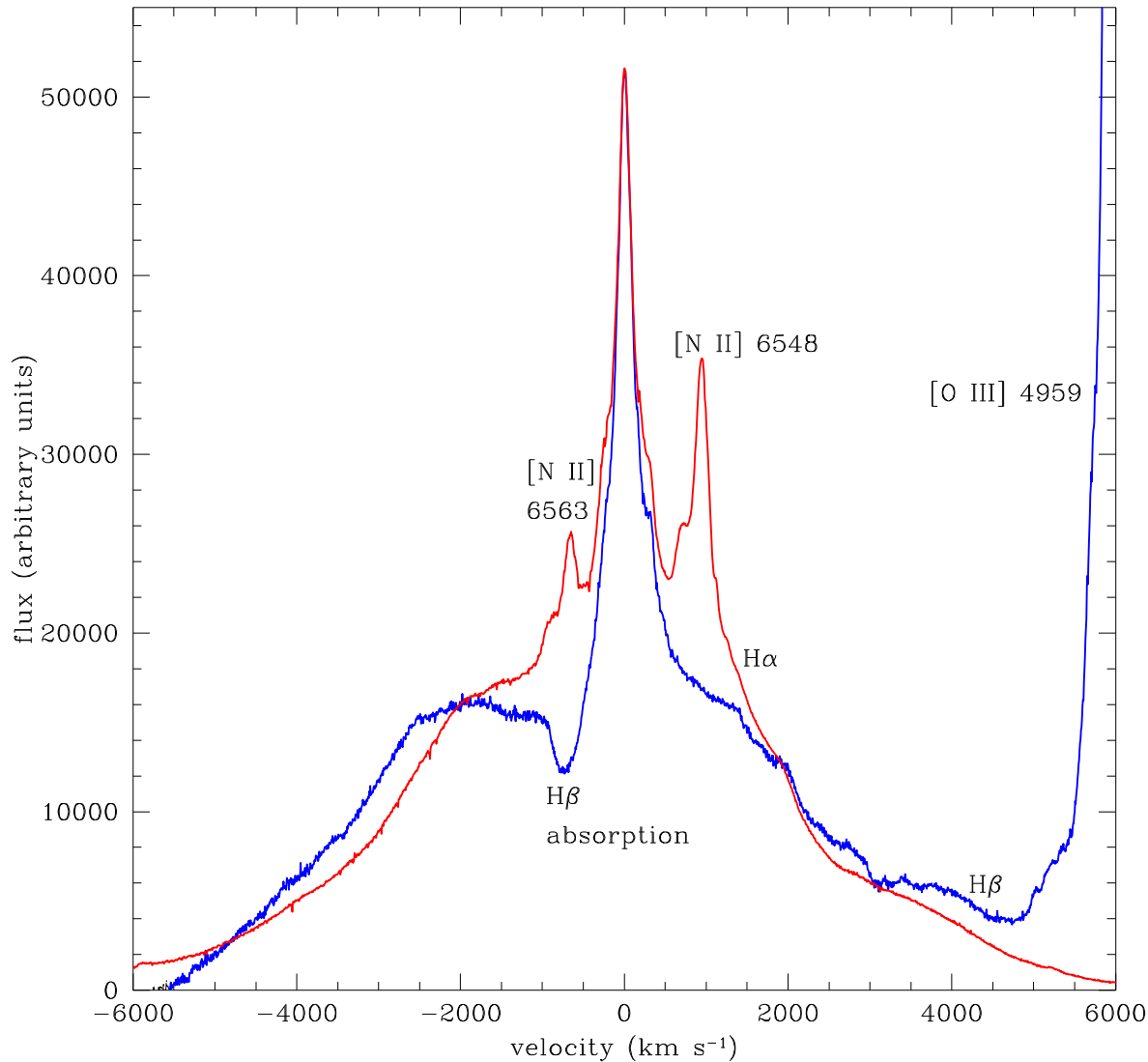
(Kaspi et al., 2005, Fig. 2)

In detail, things are more complicated, and slope is steeper than 0.5: $R \propto L^{0.67 \pm 0.05}$

\Rightarrow ionization parameter, density, and spectral shape depend somewhat on L .



What is the BLR?, I



NGC 4151 (Sy 1; Arav et al., 1998, Fig. 1)

Classical assumption: BLR is collection of cold clouds embedded in hot gas

(“two phase medium”, Krolik, McKee & Tarter 1981)

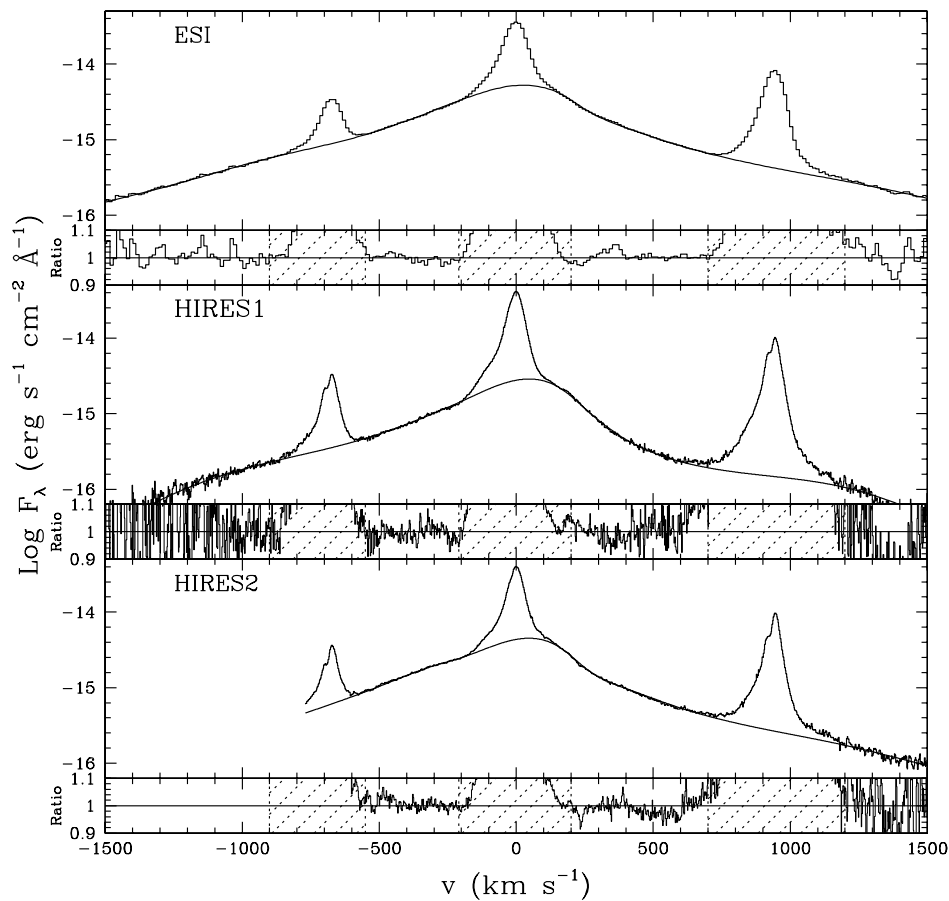
⇒ We expect to see evidence for emission from individual clouds.

Problem: BLR line profiles are *always* smooth!

⇒ Does the BLR consist of *many* small clouds?



What is the BLR?, II



(NGC 4395 Laor et al., 2006)

Observations show always smooth BLR profiles, even for lowest luminosity AGN such as NGC 4395 (the lowest luminosity Sy 1 known)

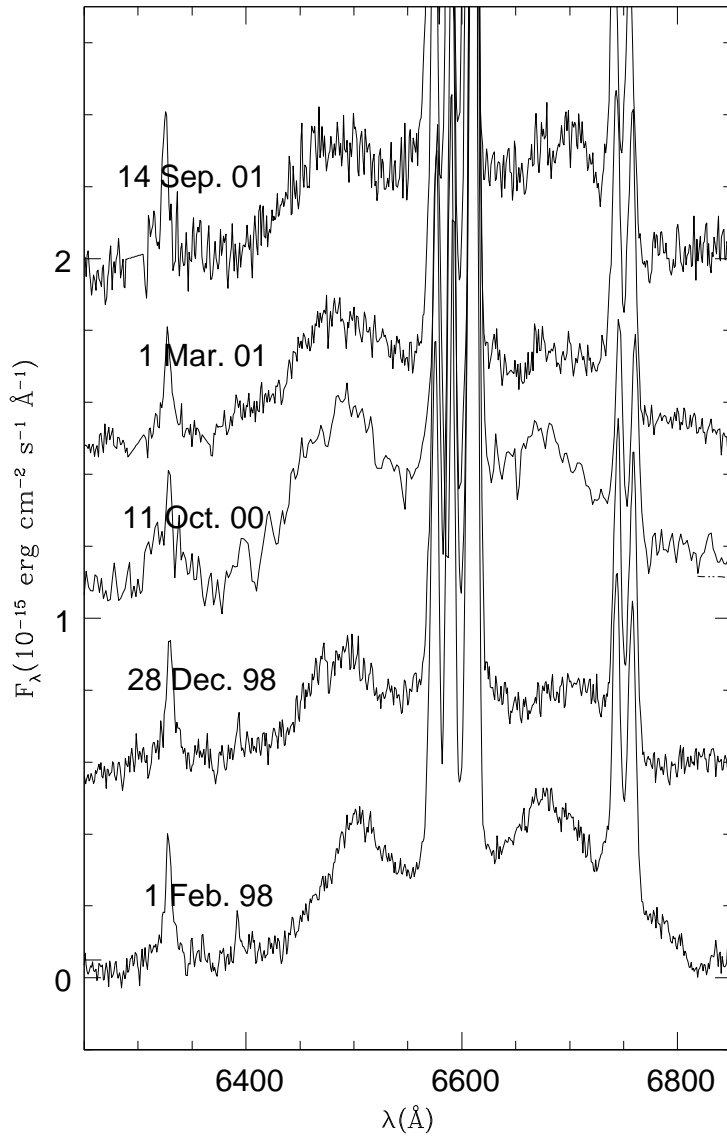
⇒ this is only possible if there is a *very large* number of clouds such that it is better to speak about a “clumpy” gas.

For NGC 4151, Arav et al. (1998) find that there must be $\gtrsim 3 \times 10^7$ clouds, for NGC 4395, $> 10^5$ clouds are required (Laor et al., 2006). Since $R_{\text{BLR}, 4395} \sim 10^{14}$ cm from reverberation, $R_{\text{cloud}, 4395} \lesssim 10^{12}$ cm, i.e., much smaller than stars.

The BLR cannot consist of individual clouds, it rather is a smooth(ish) gas cloud surrounding the BH.



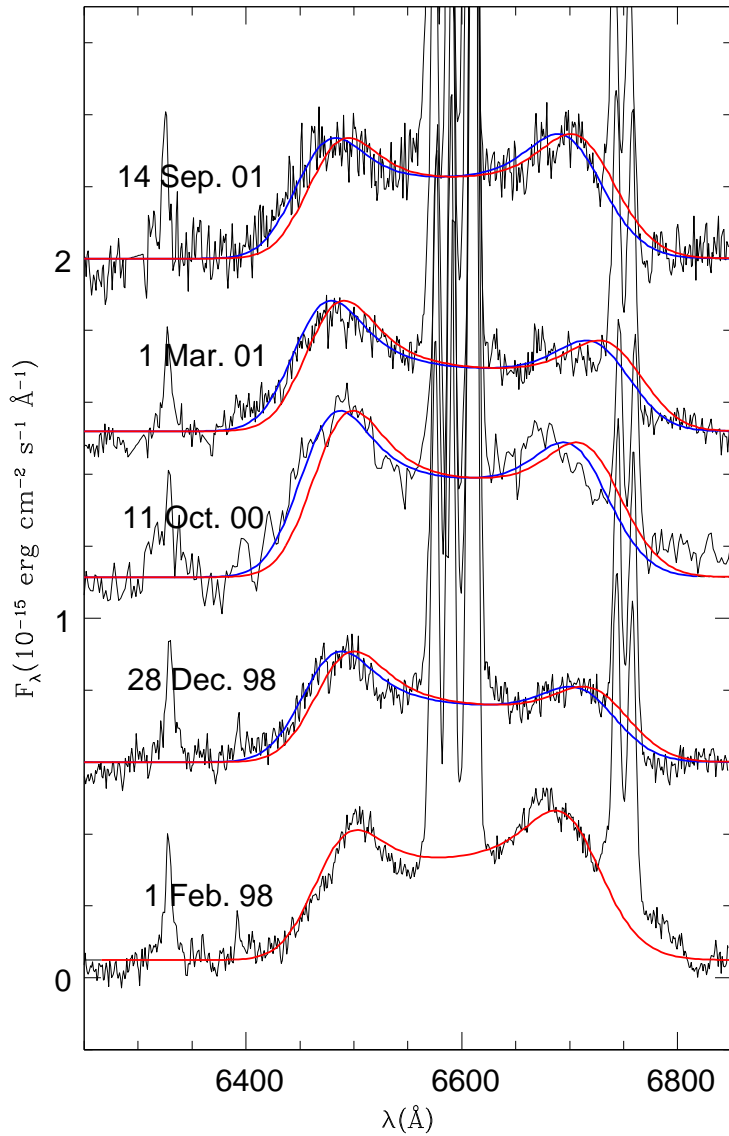
What is the BLR?, III



In some AGN BLR profiles are double humped

NGC 1097 (Sy1; Storchi-Bergmann et al., 2003, Fig. 8)

What is the BLR?, IV



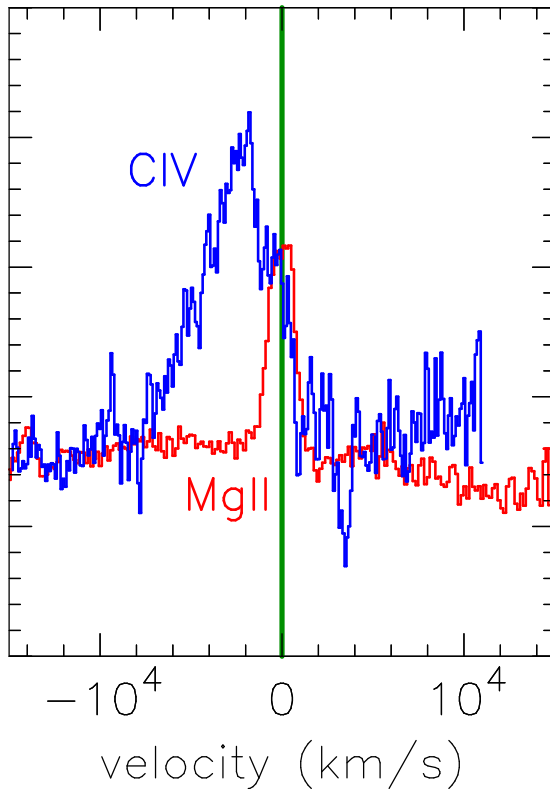
In some AGN BLR profiles are double humped
⇒ is BLR the outer edge of accretion disk?

NGC 1097 (Sy1; Storchi-Bergmann et al., 2003, Fig. 8)

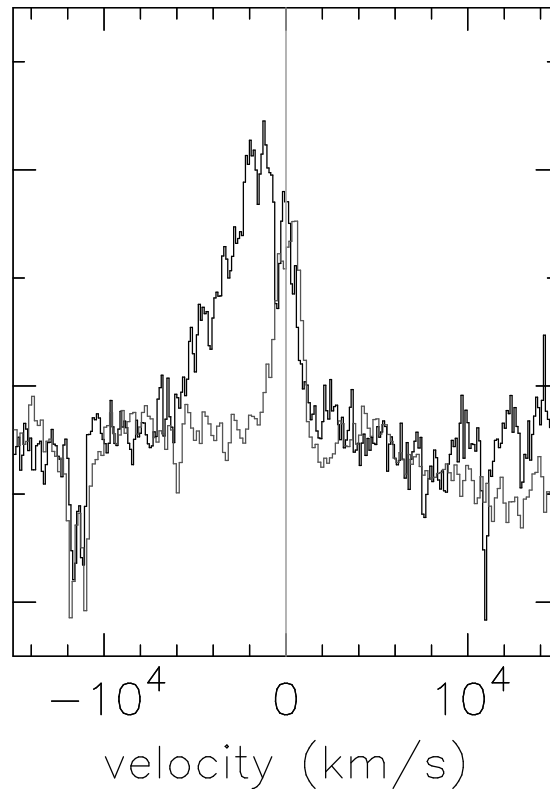


Winds

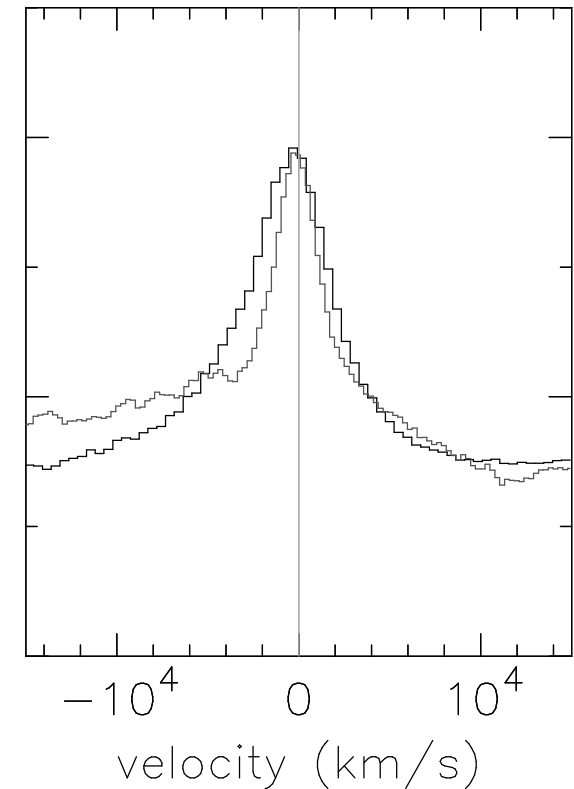
IRAS 13224-3809



1H 0707-495



Average QSO



(Leighly & Moore, 2004)

While disk emission explains part of BLR emission, not all features can be explained: Sy 1 show asymmetric line profiles: **Higher ionization lines are shifted bluewards** \implies Outflow!



Winds

There are also findings that the line blueshift increases with AGN luminosity:
evidence for radiatively driven outflows?

Is the BLR an accretion disk wind?

Driving mechanisms:

- **Electromagnetic?**

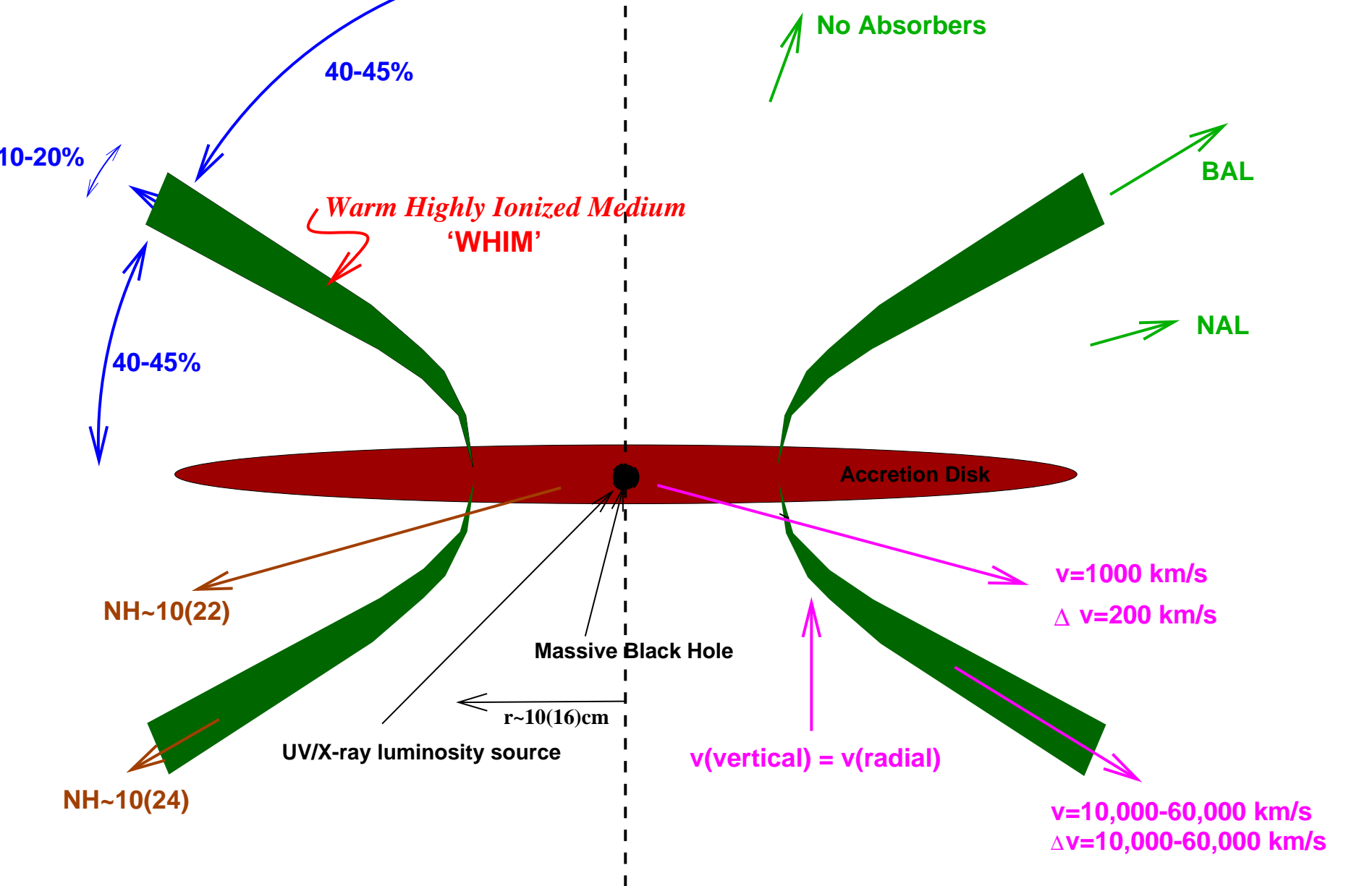
related to jet?

- **Radiatively driven?**

related to high AGN luminosity

GEOMETRY

TAXONOMY



PHYSICS

Log radial scale

KINEMATICS

(Elvis, 2000, Fig. 1)



BH Masses

Regardless of the detailed interpretation of the BLR, **measurements of the BLR allow for a (statistical) determination of the mass of the Black Hole:**

The **virial theorem** of mechanics states:

$$2T = m\Delta V^2 = \eta \cdot G \frac{mM_{\text{BH}}}{r_0} = U \quad (8.28)$$

where m mass of a test particle, r_0 : characteristic BLR radius, ΔV : **velocity dispersion**, and η : geometry dependent factor.

Since r_0 and ΔV can be measured from reverberation mapping and the line width:

$$M_{\text{BH}} = f \cdot \frac{r\Delta V^2}{G} \quad (8.29)$$

where f is a geometry dependent normalization factor, obtained from calibration measurements.

Note: For virial theorem to apply, motion of BLR must be dominated by gravity.

To derive the virial theorem, we look at a system of particles of mass m_i . The acceleration on particle i by all other particles is

$$\ddot{\mathbf{r}} = \sum_{j \neq i} \frac{Gm_j(\mathbf{r}_j - \mathbf{r}_i)}{|\mathbf{r}_j - \mathbf{r}_i|^3} \quad (8.30)$$

... scalar product with $m_i \mathbf{r}_i$

$$m_i \mathbf{r}_i \cdot \ddot{\mathbf{r}} = \sum_{j \neq i} \frac{Gm_i m_j \mathbf{r}_i \cdot (\mathbf{r}_j - \mathbf{r}_i)}{|\mathbf{r}_j - \mathbf{r}_i|^3} \quad (8.31)$$

... since

$$\frac{1}{2} \frac{d^2 \mathbf{r}_i^2}{dt^2} = \frac{d}{dt} (\dot{\mathbf{r}}_i \cdot \mathbf{r}_i) = \ddot{\mathbf{r}}_i \cdot \mathbf{r}_i + \dot{\mathbf{r}}_i \cdot \dot{\mathbf{r}}_i \quad (8.32)$$

... therefore Eq. (8.31)

$$\frac{1}{2} \frac{d^2}{dt^2} (m_i \mathbf{r}_i^2) - m_i \dot{\mathbf{r}}_i^2 = \sum_{j \neq i} \frac{Gm_i m_j \mathbf{r}_i \cdot (\mathbf{r}_j - \mathbf{r}_i)}{|\mathbf{r}_j - \mathbf{r}_i|^3} \quad (8.33)$$

Summing over all particles in the system gives

$$\frac{1}{2} \sum_i \frac{d^2}{dt^2} (m_i \mathbf{r}_i^2) - \sum_i m_i \dot{\mathbf{r}}_i^2 = \sum_i \sum_{j \neq i} \frac{Gm_i m_j \mathbf{r}_i \cdot (\mathbf{r}_j - \mathbf{r}_i)}{|\mathbf{r}_j - \mathbf{r}_i|^3} \quad (8.34)$$

$$= \frac{1}{2} \left(\sum_i \sum_{j \neq i} Gm_i m_j \frac{\mathbf{r}_i \cdot (\mathbf{r}_j - \mathbf{r}_i)}{|\mathbf{r}_i - \mathbf{r}_j|^3} + \sum_j \sum_{i \neq j} Gm_j m_i \frac{\mathbf{r}_j \cdot (\mathbf{r}_i - \mathbf{r}_j)}{|\mathbf{r}_j - \mathbf{r}_i|^3} \right) \quad (8.35)$$

$$= \frac{1}{2} \left(\sum_i \sum_{j \neq i} Gm_i m_j \frac{\mathbf{r}_i \cdot \mathbf{r}_j - \mathbf{r}_i^2}{|\mathbf{r}_i - \mathbf{r}_j|^3} + \sum_j \sum_{i \neq j} Gm_j m_i \frac{\mathbf{r}_j \cdot \mathbf{r}_i - \mathbf{r}_j^2}{|\mathbf{r}_j - \mathbf{r}_i|^3} \right) \quad (8.36)$$

$$= -\frac{1}{2} \sum_{\substack{i,j \\ i \neq j}} \frac{Gm_i m_j}{|\mathbf{r}_i - \mathbf{r}_j|} \quad (8.37)$$

Thus, identifying the total kinetic energy, T , and the gravitational potential energy, U , gives

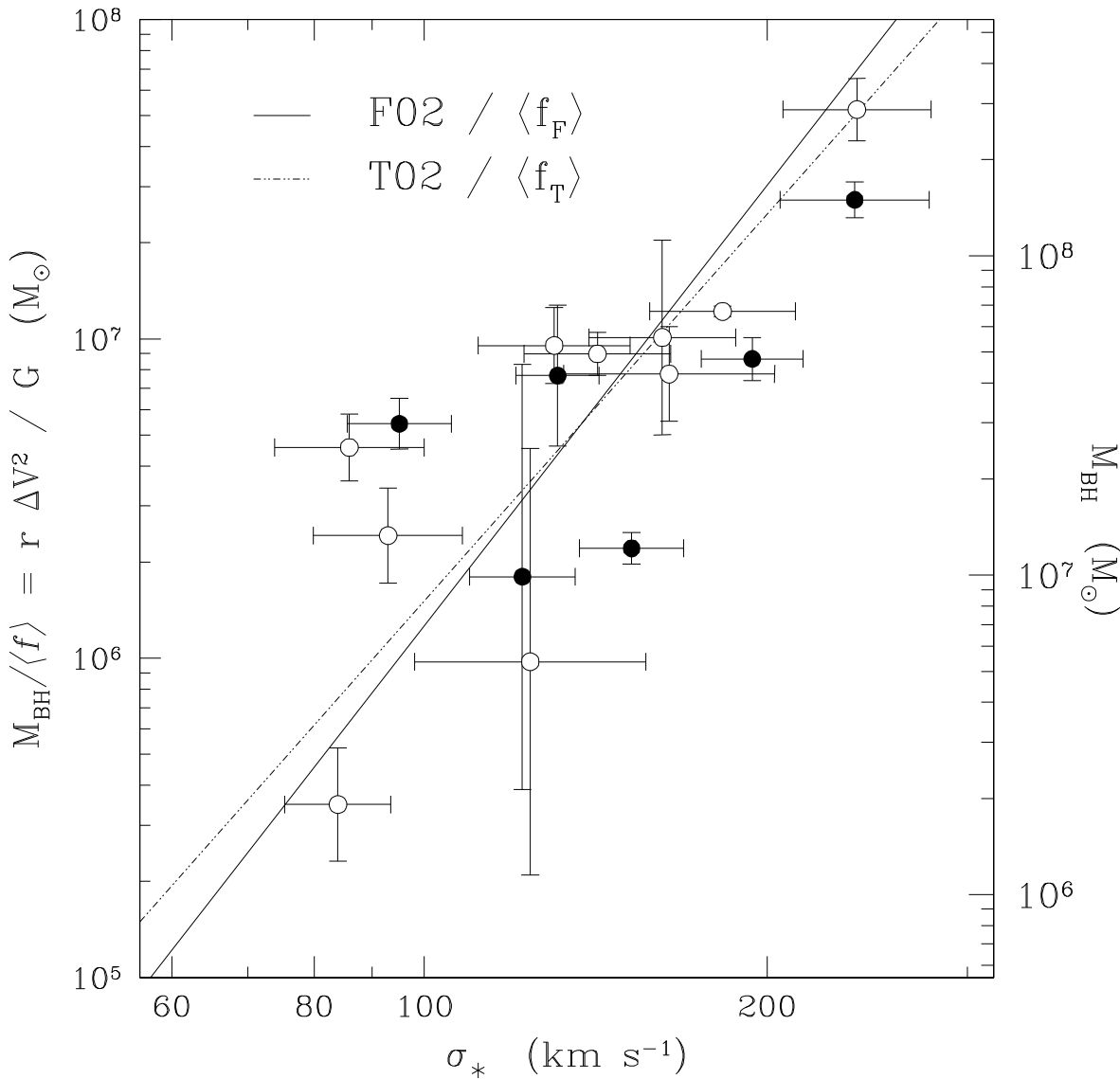
$$2T - U = \frac{1}{2} \frac{d^2}{dt^2} \sum_i m_i \mathbf{r}_i^2 = 0 \quad (8.38)$$

in statistical equilibrium.

Thus we find the virial theorem: $T = \frac{1}{2}|U|$



BH Masses



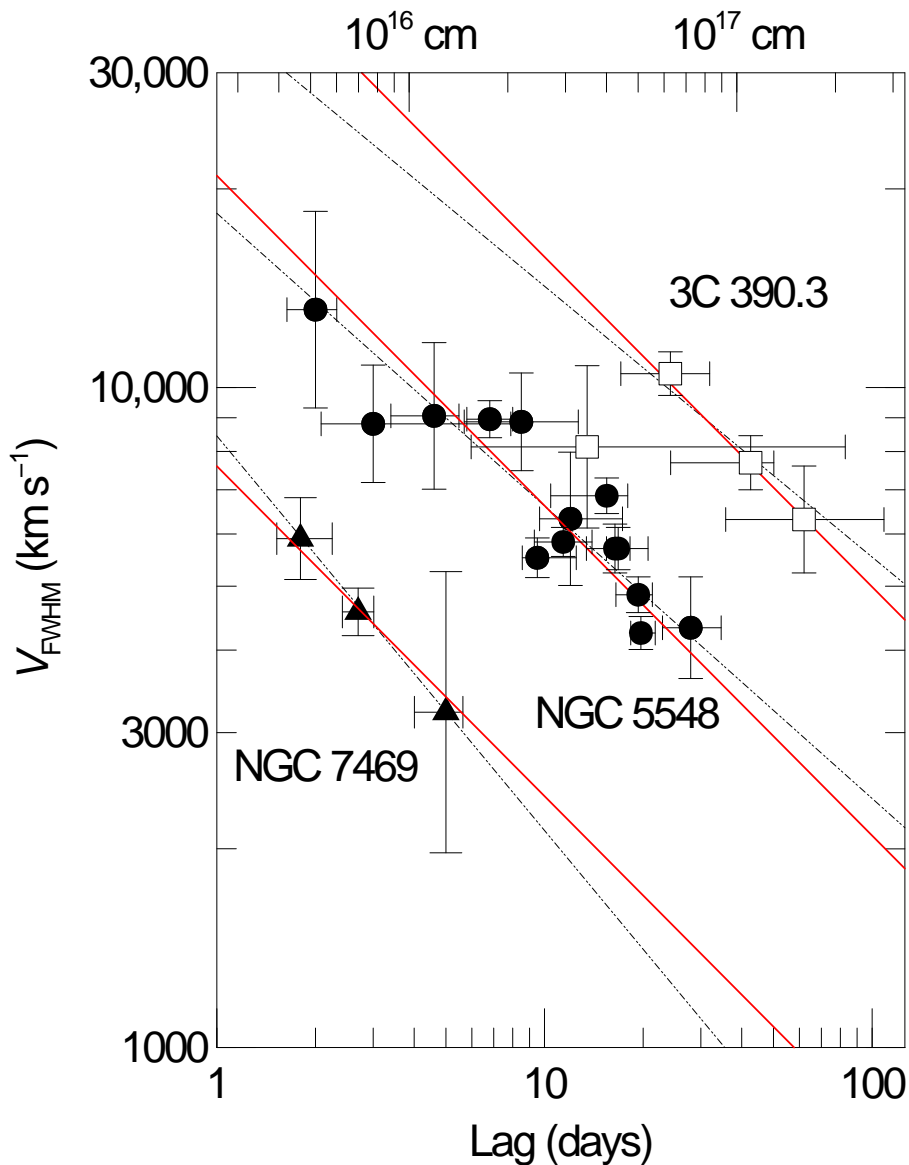
Onken et al. (2004):
Calibration of reverberation mapping based on other AGN mass determinations (M - σ -relationship, see later):

$f = 5.5 \pm 1.9$

⇒ Masses determined from reverberation mapping are exact to ~35%.



BH Masses



Since $M \propto r \Delta V^2$, for a single object ($M = \text{const.}$), **we expect** $r \propto \Delta V^{-1/2}$.

Observations: Line width versus lag scales as

$$\log V_{\text{rms}} = a + b \log c\tau \quad (8.39)$$

with $b = -1/2$, as expected!

solid lines in the figure

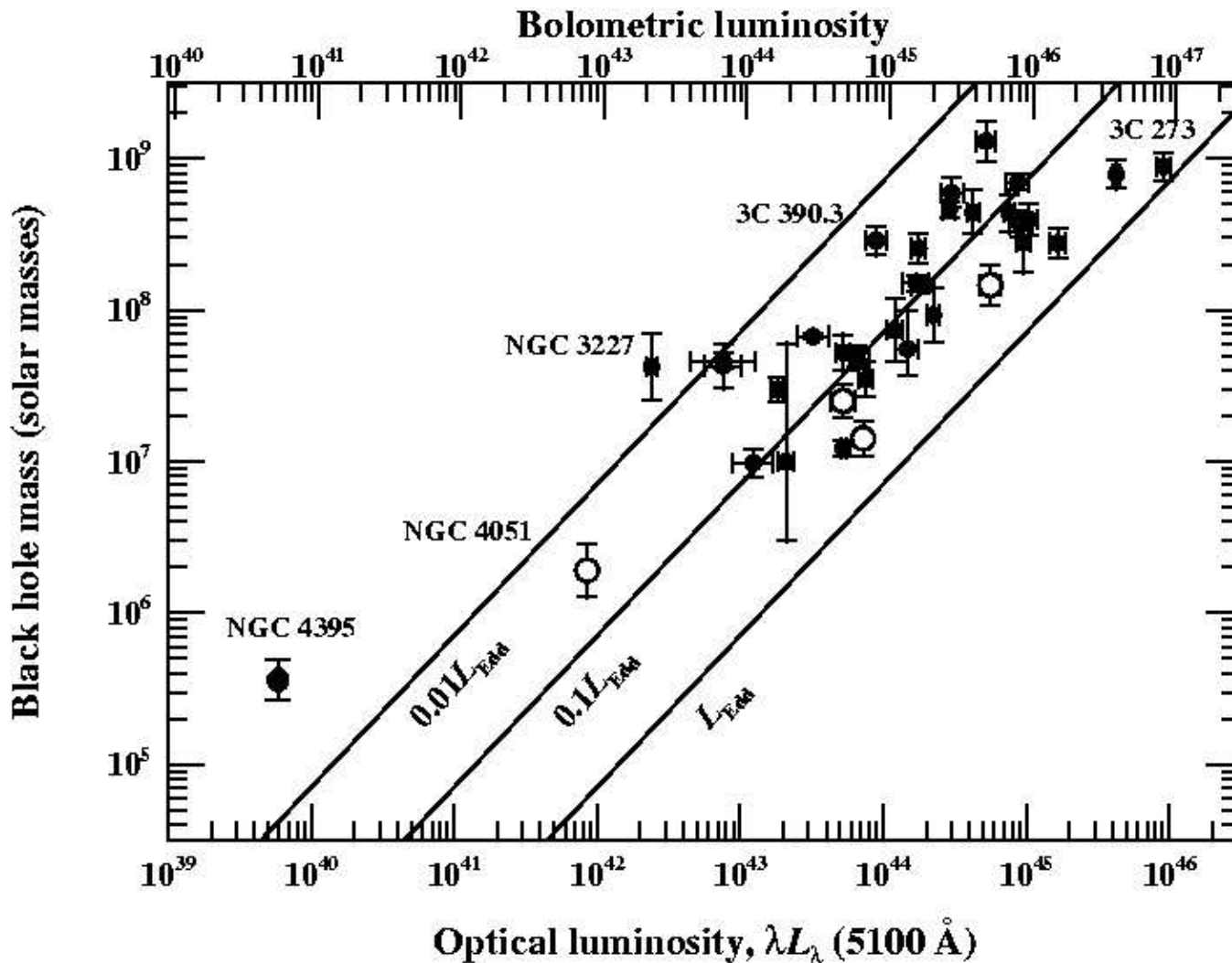
Masses obtained from lag and V (Peterson & Wandel, 2000):

- NGC 7469: $8.4 \times 10^6 M_{\odot}$
- NGC 5548: $5.9 \times 10^7 M_{\odot}$
- 3C 390.3: $3.2 \times 10^8 M_{\odot}$

(Peterson, 2001)



BH Masses



Until today: 36 AGN with reverberation measurements.
Mass-luminosity relationship: typical efficiency for AGN accretion is 10%.

Peterson (2006; Xian AGN workshop)

- Arav, N., Barlow, T. A., Laor, A., Sargent, W. L. W., & Blandford, R. D., 1998, *MNRAS*, 297, 990
- Blandford, R. D., & McKee, C. F., 1982, *ApJ*, 255, 419
- Clavel, J., et al., 1992, *ApJ*, 393, 113
- Elvis, M., 2000, *ApJ*, 545, 63
- Kaspi, S., Maoz, D., Netzer, H., Peterson, B. M., Vestergaard, M., & Jannuzi, B. T., 2005, *ApJ*, 629, 61
- Kollatschny, W., Bischoff, K., & Dietrich, M., 2000, *A&A*, 361, 901
- Krolik, J. H., McKee, C. F., & Tarter, C. B., 1981, *ApJ*, 249, 422
- Laor, A., Barth, A. J., Ho, L. C., & Filippenko, A. V., 2006, *ApJ*, 636, 83
- Leighly, K. M., & Moore, J. R., 2004, *ApJ*, 611, 107
- Onken, C. A., Ferrarese, L., Merritt, D., Peterson, B. M., Pogge, R. W., Vestergaard, M., & Wandel, A., 2004, *ApJ*, 615, 645
- Peterson, B. M., 2001, in *Advanced Lectures on the Starburst-AGN Connection*, ed. I. Aretxaga, D. Kunth, R. Mújica, (Singapore: World Scientific), 3
- Peterson, B. M., 2006, in *Physics of Active Galactic Nuclei at All Scales*, ed. D. Alloin, R. Johnson, P. Lira, Vol. 693, (Berlin, Heidelberg: Springer), 77
- Peterson, B. M., et al., 2004, *ApJ*, 613, 682
- Peterson, B. M., & Wandel, A., 2000, *ApJ*, 521, L95
- Storchi-Bergmann, T., et al., 2003, *ApJ*, 598, 956
- vanden Berk, D., Yip, C., Connolly, A., Jester, S., & Stoughton, C., 2004, in *AGN Physics with the Sloan Digital Sky Survey*, ed. G. T. Richards, P. B. Hall, 21